Shedding New Light On **MICROSCOPY**

APPLICATION NOTE

AX/AX R with NSPARC Confocal-based Super Resolution Microscope

Distortion Correction Technique with Non-linear Deconvolution Using Fluorescent Beads as Reference Data

Image Scanning Microscopy (ISM) improves spatial resolution without compromising signal intensity. When combined with deconvolution processing, ISM enables the generation of super-resolution images that surpass the traditional optical resolution limits.

However, in three-dimensional (3D) imaging, refractive index mismatches between the immersion medium of the objective lens (e.g., water, silicone, oil) and the biological sample can introduce distortions along the optical axis. This remains a challenge even with ISM-enhanced in-plane resolution.

In this Application Note, we applied Non-linear Deconvolution using point spread functions (PSFs) extracted from fluorescent beads embedded at various depths. We compared the resulting optical axial resolution with that obtained through standard Linear Deconvolution based on theoretical PSF models.

Materials & Methods

Small intestine slices were immunostained and embedded using the acrylamide-based A-ha polymer (refractive index R.I. = 1.53), developed by Prof. Shiue-Cheng (Tony) Tang's lab at National Tsing Hua University, Taiwan (Nat. Commun, 14:3395, 2023; https://www.nature.com/articles/s41467-023-39082-4). This preparation ensures high transparency, excellent refractive index uniformity, and strong resistance to photobleaching. Point spread functions (PSFs) were extracted from TetraSpeck™ microspheres (diameter: 100 nm, Thermo Fisher Scientific) embedded in custom-made RapiClear 1.53 gel (R.I. = 1.53, SunJin Lab Co., Taiwan). These extracted PSFs were used for Non-linear Deconvolution either before or after imaging of the small intestine samples.

The imaging target was peptide hormone vesicles (GLP-1) in mouse intestinal L-cells, which secrete GLP-1 to promote insulin secretion and regulate metabolism, an important focus in obesity and diabetes research. Both oil- and silicone-immersion objective lenses were used for examination. 3D datasets were acquired by Confocal and ISM modes with 0.1 µm Z-steps. We compared full width at half maximum (FWHM) measurements of vesicles processed by Linear and Non-linear deconvolution methods.

Results

Fig. 1

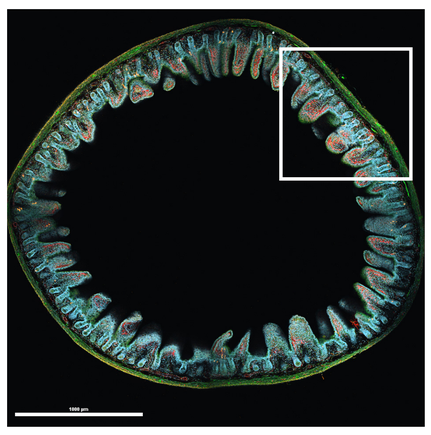

Fig. 2

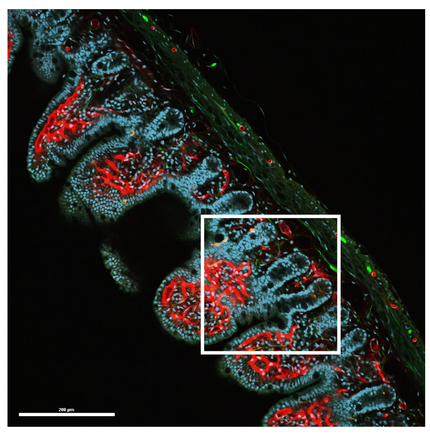

Fig. 3-a

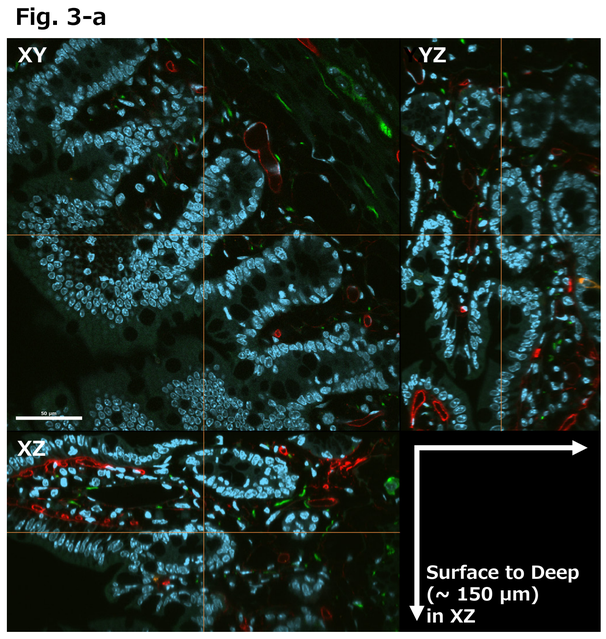

Fig. 4-a

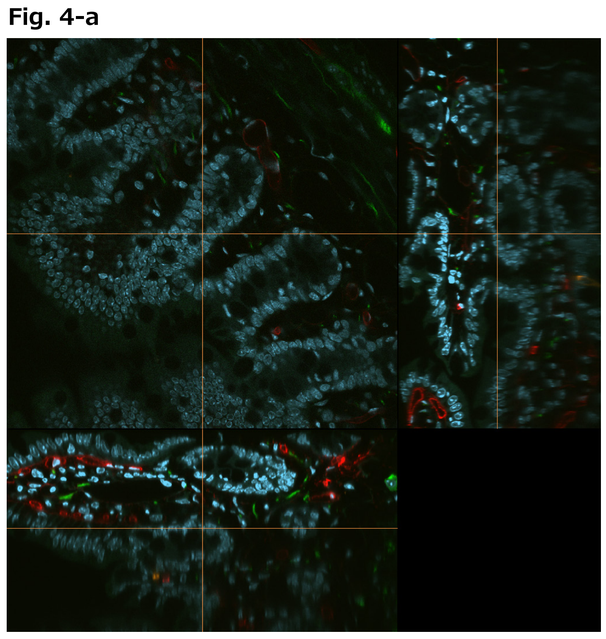

Small intestine tissue (~350 µm thick) embedded in A-ha polymer (R.I. = 1.53). Fluorescent markers: nucleus, DAPI (cyan); GLP-1 vesicles in L-cells, Alexa Fluor (AF) 488 (orange); blood vessels, AF 546 (red, perfusion labeling); nerves, AF 647 (green).

Fig. 1: Global view of a coronal slice of small intestine. 10×/0.45 objective, 2×2 stitching, pixel size 1.72 µm. scale bar = 1000 µm

Fig. 2: Zoomed area (rectangle from Fig. 1) captured with 20×/0.8 objective, pixel size 0.86 µm. scale bar = 200 µm

Fig. 3-a: Orthogonal view from rectangle in Fig. 2, captured with 60×/1.42 oil objective, pixel size 0.28 µm, Z-stack step 0.1 µm (over Nyquist sampling). scale bar = 50 µm

Fig. 3-b: Averaged PSF shapes (~20 samples) at different depths using the same settings as Fig. 3-a.

Fig. 4-a: Orthogonal view captured with 60×/1.30 silicone objective, pixel size 0.29 µm, Z-stack interval 0.1 µm (over Nyquist sampling).

Fig. 4-b: Averaged PSF shapes (~20 samples) at different depths using the same settings as Fig. 4a.

Fig. 3-b

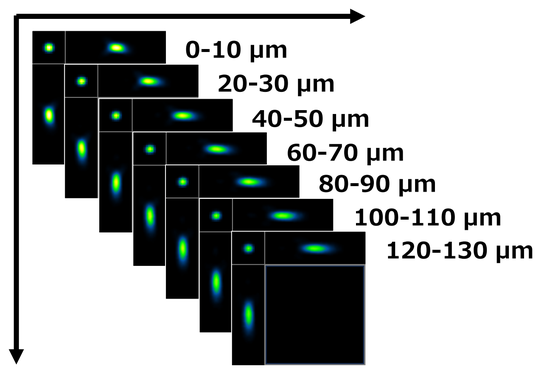

Fig. 4-b

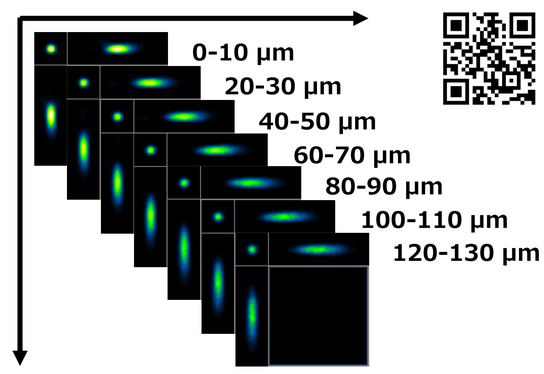

*QR movie shows the differences in brightness and resolution between oil- and silicone-immersion lenses.

Fig. 5

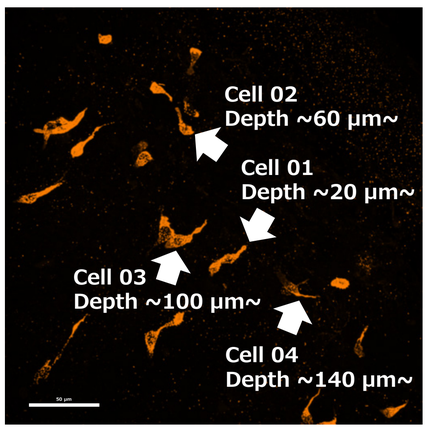

Fig. 6

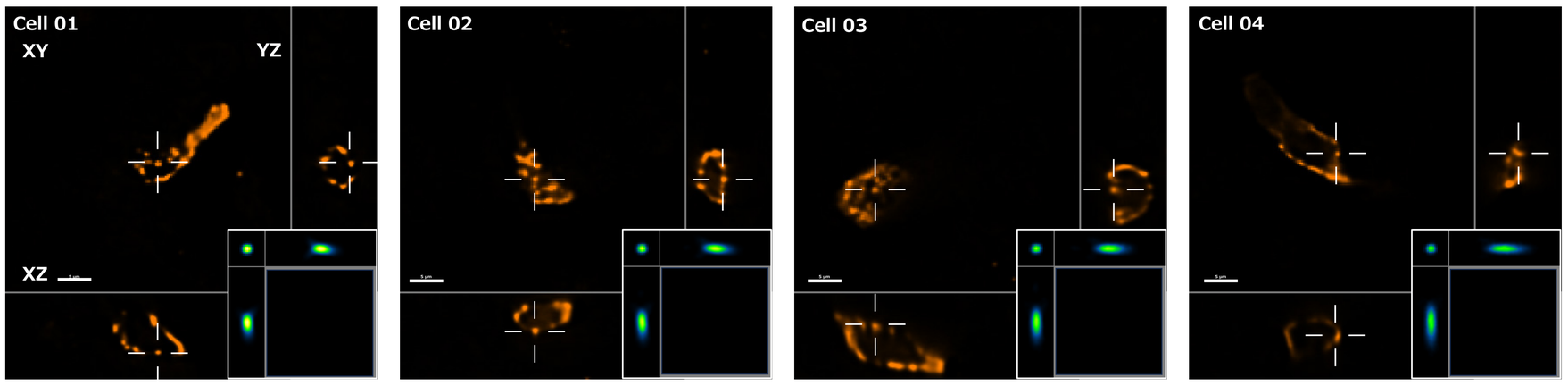

Fig. 5: Maximum intensity projection of L-cells. Volume data corresponding to the area shown in Fig. 3-a. scale bar = 50 µm

Fig. 6: Orthogonal views of Non-linear Deconvolution images of L-cells (Confocal). GLP-1 vesicles in Cell 01, Cell 02, Cell 03, and Cell 04. Crosshairs indicate the locations where FWHM measurements were performed. Inserted images show depth-matched PSFs extracted from Fig. 3-b. scale bar = 5 µm

Table 1

GLP-1 Cell	Depth from glass surface	Objective-lens	FWHM of std DCV / psf DCV in XZ	FWHM of std DCV / psf DCV in YZ
Cell 01	~17um~	PA60x/1.42 Oil	0.086 / 0.075	0.092 / 0.075
		Silicone60x/1.30	0.105 / 0.103	0.100 / 0.096
Cell 02	~62um~	PA60x/1.42 Oil	1.657 / 0.961	1.165 / 0.874
		Silicone60x/1.30	1.996 / 1.525	1.841 / 1.502
Cell 03	~100um~	PA60x/1.42 Oil	1.701 / 1.098	1.454 / 1.173
		Silicone60x/1.30	1.848 / 1.611	1.894 / 1.590
Cell 04	140um~	PA60x/1.42 Oil	1.899 / 1.396	1.506 / 1.237
		Silicone60x/1.30	4.020 / 3.212	4.000 / 3.200

Table 2

GLP-1 Cell	Depth from glass surface	Objective-lens	FWHM of std DCV / psf DCV in XZ	FWHM of std DCV / psf DCV in YZ
Cell 01	~17um~	PA60x/1.42 Oil	0.456 / 0.454	0.057 / 0.454
		Silicone60x/1.30	0.620 / 0.720	0.788 / 0.866
Cell 02	~62um~	PA60x/1.42 Oil	0.869 / 0.821	1.083 / 0.748
		Silicone60x/1.30	2.120 / 1.735	1.863 / 1.722
Cell 03	~100um~	PA60x/1.42 Oil	0.954 / 0.954	0.876/ 0.708
		Silicone60x/1.30	1.429 / 1.342	1.723 / 1.648
Cell 04	140um~	PA60x/1.42 Oil	0.617 / 0.600	0.561 / 0.620
		Silicone60x/1.30	-	-

Table 1. FWHM Measurements of GLP-1 Vesicles by Confocal Imaging. We measured the GLP-1 vesicle size along the optical axis (n=5). This table presents FWHM values in XZ and YZ planes for each L-cell shown in Fig. 6, comparing standard Linear Deconvolution (std DCV) and Non-linear Deconvolution (psf DCV) processed with Lucy-Richardson (10 iterations). Images were acquired using Confocal mode with oil- and silicone-immersion objectives. **Table 2. FWHM Measurements of GLP-1 Vesicles by ISM Imaging.** Table 2 presents the FWHM values for the same vesicles measured in ISM mode, comparing std DCV and psf DCV approaches. All processing was performed with the Lucy-Richardson algorithm (10 iterations). Values highlighted in red indicate possible deviations due to sample drift or external vibrations during ISM imaging.

Fig. 7

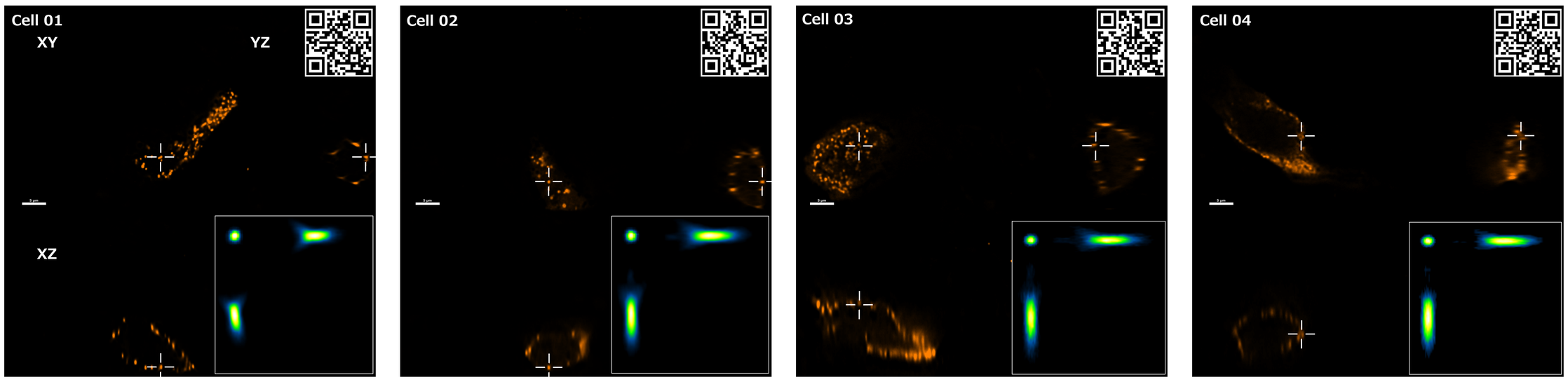

Fig. 7: Orthogonal views of Non-linear Deconvolution images for L-cells imaged by ISM mode. (Cell 01, 02: pixel size 0.041 µm; Cell 03, 04: pixel size 0.032 µm, Z-step 0.1 µm.)
Inserted images show extracted PSF shapes corresponding to each L-cell depth. scale bar = 5 µm
*(QR codes link to movies showing GLP-1 particle Z-stacks: Left = std DCV, Right = psf DCV.)

Fig. 8

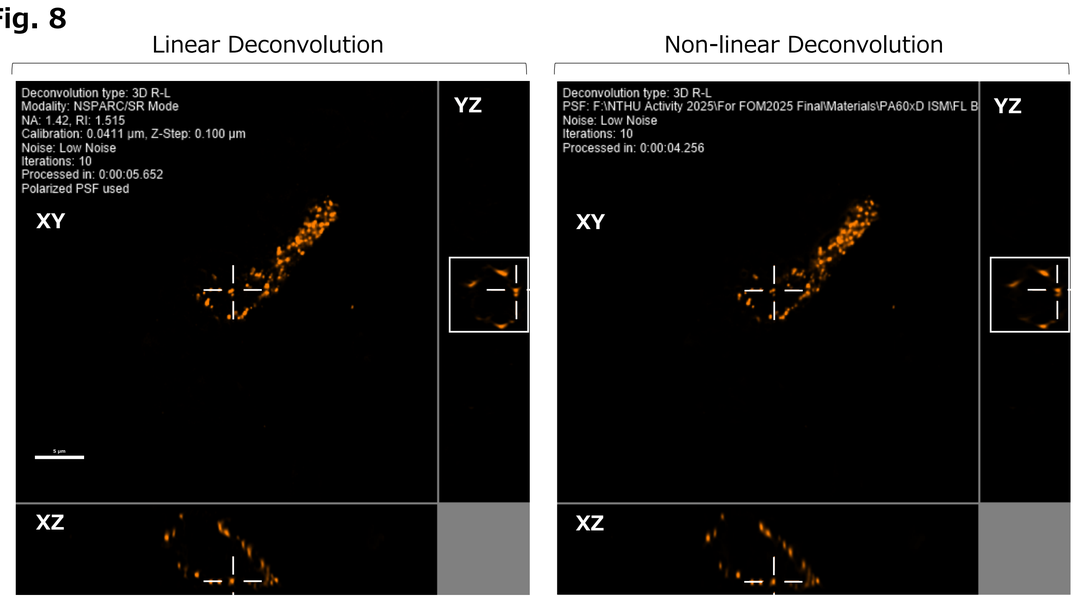

Fig. 9

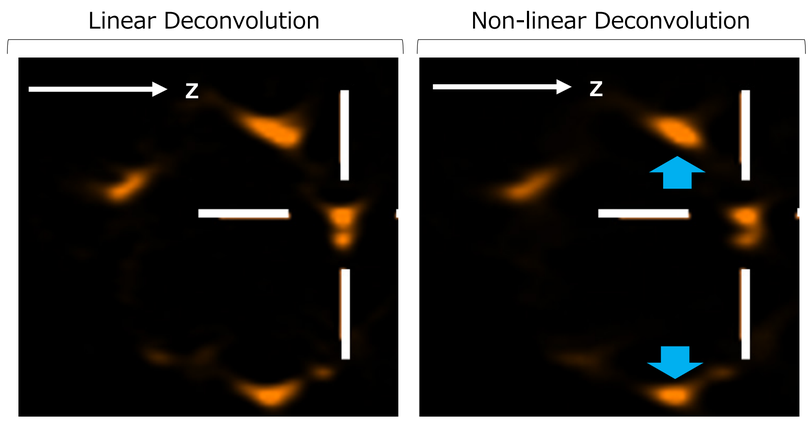

Fig. 8: Comparisons of orthogonal views of Linear and Non-linear Deconvolution images for L-cells imaged by ISM mode. (Cell 01; images on Fig. 7 are reused for Non-linear deconvolution images). scale bar = 5 µm
Fig. 9: Close-up views of YZ images on Fig. 8. Regions indicated by white rectangles are shown. As indicated by the blue arrows, after non-linear deconvolution processing, the elongation of red bright spots in the axial direction is suppressed

Summary

As demonstrated in Figs. 3 and 4, refractive index mismatch between the sample and immersion medium significantly impacts imaging performance. Oil immersion (R.I. = 1.52) closely matched the sample refractive index (R.I. = 1.53), maintaining brightness and resolution up to depths of 150 µm, whereas silicone immersion (R.I. = 1.41) led to a marked decline in imaging quality at shallower depths.

Thus, although transparency techniques improve deep tissue imaging, optimizing the refractive index match between the sample and objective immersion medium remains critical for achieving high-resolution results. Tables 1 and 2 confirm that Non-linear Deconvolution using depth-matched PSFs outperforms Linear Deconvolution, especially under conditions of refractive index mismatch.

However, the high resolving power of ISM requires careful management of vibrations and sample drift to avoid artifacts, as noted in Table 2.

With ISM rapidly becoming the new standard over traditional Confocal microscopy, enhancing axial resolution through Non-linear Deconvolution represents an essential advancement for 3D biological imaging.

Appendix: Protocol of PSF Extractor

The PSF Extractor is a tool for deconvolution, designed to correct for spherical aberration that arises from refractive index mismatches between the sample and the objective lens immersion medium. It achieves this by extracting depth-dependent PSFs directly from measured bead samples. To effectively utilize this feature, follow the step-by-step guide provided below.

Step 1: Determine the depth of the actual sample from the glass interface.
Step 2: Acquire Z-stack images of fluorescent beads at corresponding depths, using the same pixel size and Z-step as your sample.
(Note: Select bead diameters appropriate for the objective lens magnification.)
Step 3: Open "PSF Extractor" (Top Menu > Deconvolution > "Extract PSF"), select bead diameter and number of layers.
Step 4: Confirm PSF shapes in Orthogonal view, then save the PSF file.
Step 5: Extract the relevant channel from your sample image for deconvolution.
Step 6: In the "3D Deconvolution" window, set General parameters, then import the saved PSF file under the Advanced tab.

Acknowledgments

Special thanks to Prof. Shiue-Cheng (Tony) Tang at National Tsing Hua University, Taiwan for providing super-resolution optimized samples with uniform refractive index and high transparency using the A-ha polymer embedding technique.

Edited by Ryu Nakamura, Shingo Nagawa Nikon Corporation